PERGAMON

International Journal of Multiphase Flow 27 (2001) 1753–1767

International Journal of Multiphase Flow

www.elsevier.com/locate/ijmulflow

# An experimental study of critical heat flux (CHF) in microgravity forced-convection boiling

Yue Ma [a], J.N. Chung [b,*]

[a] School of Mechanical and Materials Engineering, Washington State University, Pullman, WA 99164-2920, USA
[b] Department of Mechanical Engineering, University of Florida, Gainesville, FL 32611-6300, USA

Received 6 July 2000; received in revised form 2 April 2001

**Abstract**

Pool and forced-convection boiling of FC-72 was conducted in earth gravity and microgravity. A platinum wire heater was used to generate bubbles and provide simultaneous measurement of the heater surface mean temperature. An electrical circuit was built to control the temperature of heater surface. Boiling curves of FC-72 for different flow rates were obtained in the experiment. By using photographic visualization, it was observed that the microgravity environment decreased the critical heat flux (CHF) significantly and force the boiling to switch to transition or film regime. With an increase of the flow rate, the CHF increased and the boiling curves moved upward in both terrestrial gravity and microgravity. In this study, it was also found that the forced convection tends to offset the microgravity effect on CHF when the flow rate was sufficiently high. © 2001 Published by Elsevier Science Ltd.

*Keywords:* Forced-convection boiling; Critical heatflux; Microgravity

## 1. Introduction

The critical heat flux (CHF) represents an important point on the boiling curve. An accurate prediction of the CHF has a number of useful and practical applications on the improvement of the efficiency for boiling heat transfer equipment.

Zuber (1958) through a hydrodynamic stability analysis and Kutateladze (1948) through a dimensional analysis, obtained the following equation which was often used to predict the CHF of saturated pool boiling in terrestrial gravity:

$$q''_c = C_{max} h_{LG} \left[\sigma \rho_G^2 (\rho_L - \rho_G) g\right]^{1/4}, \tag{1}$$

* Corresponding author.

0301-9322/01/$ - see front matter © 2001 Published by Elsevier Science Ltd.
PII: S0301-9322(01)00031-3

where $q''_c$ is the CHF for saturated boiling, $C_{max}$ is a constant based on the heater geometry, $h_{LG}$ is the latent heat of vaporization, $\sigma$ is the surface tension coefficient, $\rho_G$ is the density of vapor, $\rho_L$ is the density of liquid, and $g$ is the gravitational acceleration.

Ivey and Morris (1966) studied the effect of liquid-phase subcooling on the CHF in pool boiling. They found that the CHF would increase linearly with the degree of subcooling and developed a correlation equation as follows:

$$\frac{q''_{c,sub}}{q''_c} = 1 + 0.1\left(\frac{\rho_G}{\rho_L}\right)^{1/4} Ja, \tag{2}$$

where $Ja$ is the Jacob number defined as

$$Ja = \frac{\rho_L c_p \Delta T_{sub}}{\rho_G h_{LG}}, \tag{3}$$

$q''_{c,sub}$ is the CHF with subcooling, $q''_c$ is the CHF at saturated condition, $\Delta T_{sub}$ is the degree of subcooling, and $c_p$ is the specific heat of the liquid.

Haramura and Katto (1983) conducted CHF experiments on a flat surface heater and a cylinder of 1 mm diameter in a cross-flow of water, R-133, and R-12. After analyzing the CHF data obtained for saturated boiling, together with other existing data for cylinders of $D = 0.81$–$6.5$ mm, they found that the effect of heater geometry can be grouped into a single coefficient $C_G$ and developed a semi-empirical correlation to predict the CHF at a sufficiently high fluid velocity:

$$\frac{q''_c}{Gh_{LG}} = C_G\left(\frac{\rho_G}{\rho_L}\right)^{0.467}\left(\frac{\sigma\rho_L}{G^2L}\right)^{1/3}, \tag{4}$$

where $G$ is the bulk mass flux, $L$ is the length of the plate in the flow direction for a flat plate heater or the diameter for a cylinder in cross-flow, and $C_G$ is 0.175 for a flat plate heater and 0.151 for a cylinder, respectively.

Many studies on boiling in microgravity were focused on nucleate boiling. Keshock and Siegel (1964) performed a study of bubble growth, departure, and dynamics during nucleate boiling of saturated aqueous-sucrose solutions in reduced gravity. Bubble departure was found to be governed by buoyancy, inertial, and surface tension forces with viscous drag being of little significance. For rapidly growing bubbles, the inertial force is sufficiently large to overcome the surface tension force. For slowly growing bubbles the surface tension force dominates the inertial force and bubble departure is dependent on buoyancy. Weinzierl and Straub (1982) conducted an experimental investigation of subcooled nucleate pool boiling with R-113 in a microgravity level of $(a/g = 10^{-4})$ for 350 s during a rocket flight. A platinum wire was used to test three different heat fluxes. The heat transfer coefficients under microgravity at low heat fluxes were found to be equal to or greater than the terrestrial values. Cinematography results showed that vapor bubbles moved along the heated wire in random directions. Coalescence of bubbles helped the removal from the wire. Merte et al. (1993) have performed several experiments to study the effect of body forces on boiling heat transfer in microgravity. They explained that nucleate boiling would be enhanced if buoyancy or some other forces act to hold vapor bubbles near the heater surface while simultaneously permitting rewetting of the heater surface to prevent burnout. Nucleate boiling and rewetting are sustained by the surface tension effects at the liquid–vapor-heater contact line.

There were very few investigations on the CHF of pool boiling in microgravity and we did not find any published results for the CHF in microgravity forced-convection boiling. Usiskin and Siegel (1961) used a counterweighted platform where they could adjust the effective gravity field on the boiling system. The study showed that the CHF for water varied according to the 1/4 power of gravity. Moehrle (1977) performed terrestrial and microgravity pool boiling heat transfer experiments in the presence of a standing acoustic wave from a platinum wire resistance heater using degassed FC-72 Fluorinert liquid. He found that the CHF would generally decrease in microgravity. Compared with the boiling curve in terrestrial gravity, the boiling curves in microgravity for nucleate boiling region were shifted to the right and they would shift downward in the film boiling regime. His results also showed that the applied acoustic field enhanced boiling heat transfer and increased CHF in microgravity and terrestrial environments.

The objective of this paper is to provide experimental data and flow visualization results for forced-convection boiling over a constant-temperature platinum wire heater in microgravity. Specifically, complete boiling curves in terrestrial gravity and microgravity for various forced-flow conditions are presented. A photographic observation of flow boiling bubbles is introduced to facilitate physical understanding.

## 2. Experimental apparatus

Pool and forced-convection boiling experiments were conducted in both earth gravity and microgravity. The microgravity environment was obtained in the 2.1-s drop tower at the Washington State University with effective accelerations on the order of $10^{-4}g$. The flow boiling apparatus consists of a pump, preheater, boiling test section, condenser, lighting video and data acquisition system as shown in Ma and Chung (1998, Fig. 1). The maximum mean velocity over the heater surface can reach up to 35 cm/s. According to the catalog information and calibration using a CCD video camera, the uncertainty of flow meter is $\pm 4\%$ full scale ($\pm 1.4$ cm/s), and the level of fluctuations during repeat tests is $\pm 1\%$ full scale ($\pm 0.35$ cm/s). In the experiment, the flow rate was varied from 6.5 to 30 cm/s. The bulk fluid temperature was set at 30°C. Due to the heating from a running pump and a light bulb, the system temperature range is about $30 \pm 2$°C during the experiment. In our study, the system was sealed from the surroundings and the system pressure was measured at $112 \pm 3$ kPa. The system pressure was higher than that of the local atmosphere. This is because of the hydrostatic pressure head and the evaporation of the working fluid. The boiling point of the fluid used in our experiment was measured at 56°C by a thermal couple. Therefore, the degree of subcooling in the experiment was $26 \pm 2$°C. The visualization study was performed using a CCD camera with a frame rate of 1/30 s, and a shutter speed of 1/1000 s.

A platinum wire heater was used for all experiments. The 99.99% pure and annealed platinum wire was 0.01 in. in diameter and 2 cm in length. The ends of the platinum wire were connected to two copper wires used to supply power to the heater and to measure the voltage drop across the heater. A large heater length to diameter aspect ratio is commonly used to reduce the effect of conduction losses (You et al., 1990). An effective aspect ratio of 50:1 was considered to be large enough. In this study, the ratio is 80:1. The heater wire was placed horizontally and in a cross-flow condition for all the experiments.

A constant-temperature controller was designed and built by Rule (1997) at the Washington State University. This device allows the temperature of the heater to be controlled independently rather than the power input. This is necessary when studying the CHF and boiling curve because temperature control of the heater makes it possible to obtain the experimental data for the transition boiling. The mean temperature of the platinum wire is controlled by an electronic device similar to what is used in a hot-wire anemometry. The circuit design, the operational principles of the temperature controller, and the entire data acquisition system are documented in Ma (1998).

In the experiment, FC-72, a Fluorinert, was chosen as the working fluid because it is clear, colorless, odorless, non-flammable, and non-explosive. This fluid also has the benefits of low toxicity, thermal and chemical stability, and compatibility with metals and plastics. However, because of the high solubility of dissolved gases in FC-72, degassing is necessary. We decided to perform the degassing by simultaneously drawing a vacuum and boiling the fluid. Before each experiment, we performed magnetic stirring while drawing vacuum for 15 min and then followed by continuous boiling for 5 min, which turned out to be quite effective. The dissolved gas level in our working fluid was determined by comparing our data with those of You et al. (1995) in the boiling incipience probability experiment. You et al. (1995) reported a study on boiling incipience probability (the fraction of the total case that successfully initiate nucleate boiling, for example, when the degree of superheat is raised to 24 K, two out of 10 cases have failed to boil, a probability of 80% is registered) for various dissolved gas pressures ($p_g = 3.6$, 50 and 104 kPa). For $p_g = 3.6$ kPa, You et al. (1995) indicated that their system is almost dissolved gas free. For $p_g = 3.6$ kPa, the dissolved gas in the liquid should be less than 0.0025 mole/mole. As shown in Ma and Chung (1998, Fig. 2), our data agrees well with those of You et al. (1995) for $p_g = 3.6$ kPa in the boiling incipience probability study. The favorable comparison implies that our working fluid is almost dissolved gas free and the degassing in a vacuum can efficiently remove the dissolved gas in the liquid.

## 3. Experimental procedure

For each experiment, we first set up the required hardware and software for data acquisition. These included the video system and the airbag deceleration system of the drop tower. Then we performed the single point calibration for the platinum wire heater, which is required every time the heater has not been used for more than 24 h. After setting the surface temperature and the flow rate using the calibration charts, the boiling system was hoisted up to the release position and the pump was turned on. The heater power was turned on only 3 s before the release in order to minimize the free-convection effects. It was determined that a 3-s heating period is long enough to establish a steady bubble generation pattern and therefore a steady boiling process on the heater surface. Additional verification is shown in Fig. 8 where the heat flux has developed a steady pattern before the experiment is dropped. Also it was estimated that the free-convection effects established during the 3-s period would be swept downstream from the heater surface in 0.1–0.2 s for most of the flow rates in our experiment. Therefore, we believe the buoyancy effects are negligible in our experiment.

## 4. Results and discussion

### 4.1. Gravity driven terrestrial pool boiling

In order to verify our experimental system, terrestrial natural convection and nucleate pool boiling were performed and results were compared with those available in the open literature. Fig. 1 presents the comparisons between present results and existing empirical correlations. The natural convection data are compared to the well-known correlation (5) developed by Churchill and Chu (1975) for flow over a horizontal cylinder:

$$Nu_D = 0.36 + \frac{0.518\,Ra_D^{1/4}}{\left[1 + (0.559/Pr)^{9/16}\right]^{4/9}}, \tag{5}$$

where $Nu_D$ is the average Nusselt number. The Prandtl number is defined as $Pr = v/\alpha$, where $v$ and $\alpha$ are the kinematic viscosity and thermal diffusivity, respectively. The Rayleigh number is defined as

$$Ra_D = \frac{g\beta(T_{\text{wall}} - T_{\text{bulk}})D^3}{v\alpha}, \tag{6}$$

where $\beta$ is the volume thermal expansion coefficient, and $D$ is the diameter of the wire. $T_{\text{wall}}$ and $T_{\text{bulk}}$ are the heater surface temperature and the liquid bulk temperature, respectively. The Rayleigh number was determined to be well within the laminar regime ($10^{-6} < Ra_D < 10^9$). The heat transfer coefficient and the heat flux were calculated from the following equations:

$$h = \frac{k}{D}Nu_D, \tag{7}$$

$$q'' = h(T_{\text{wall}} - T_{\text{bulk}}), \tag{8}$$

where $k$ is the thermal conductivity of the fluid.

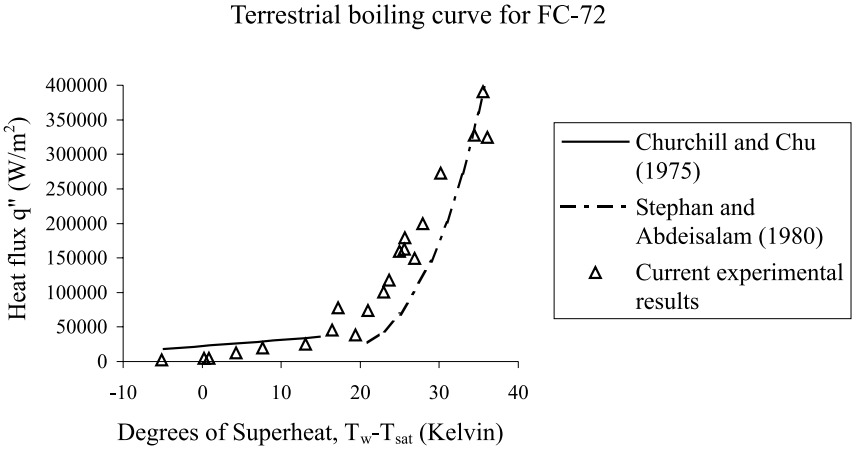


Fig. 1. Comparison between present results and existing correlations for pool boiling.

The nucleate boiling data is compared to the correlation developed by Stephan and Abdelsalam (1980):

$$q'' = [0.9(T_w - T_{sat})]^{1/0.255}. \tag{9}$$

Film boiling data were not compared to any known correlation since several thermodynamic properties for the FC-72 vapor were not available.

In general, our data agree well with the two correlations. For the natural convection regime, our data are slightly lower, which is due to the lack of detailed information on the temperature dependence of FC-72 thermal properties. For nucleate pool boiling, our data are higher for the lower heat flux portion. This is because our experiments were under subcooled condition and the correlation of Stephan and Abdelsalam (1980) is based on saturated pool boiling.

In Fig. 2, the experimental data for the entire terrestrial gravity pool boiling curve are given by diamond and square marks. The diamond ones were obtained when the temperature of heater was turned up, while the square ones when turned down. In this boiling curve, the onset heat flux of nucleate boiling is around 50,000 W/m$^2$ and the corresponding superheat is 20 K. The CHF is about 400,000 W/m$^2$, which is eight times of the onset heat flux. However, the superheat at CHF is only 40 K. The transition boiling portion is also presented as a result of using the temperature-controlled heater. It was found that the minimum heat flux is about 150,000 W/m$^2$, which is three to four times of the onset heat flux. The superheat for the minimum heat flux is 80 K. Fig. 2 also shows another experimental boiling curve reported by Moehrle (1977) who conducted his experiment under the same conditions as the present study except that he used a longer wire heater. The two boiling curves agree very well in most regions except in the film boiling portion. This might be caused by the end effect of the heater that is important only for film boiling. It is therefore important to note that, the shorter heater used in the present study is suitable for the CHF, which is less sensitive to the length of the heater.

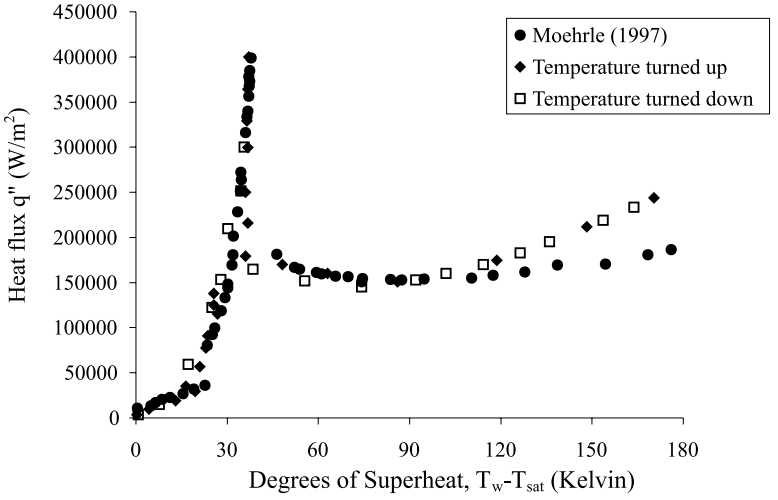


Fig. 2. Pool boiling curve of FC-72 in terrestrial gravity.

### 4.2. Forced-convection terrestrial boiling

Terrestrial gravity forced-flow boiling experiments were performed to determine the effects of forced convection on heat transfer and also to further verify the reliability of the experimental system. It is generally agreed that the influence of forced convection on boiling is the improvement of heat transfer. But the flow is particularly effective in raising the CHF. Lienhard (1988) provided a thorough literature review for the effect of cross-flow over a cylinder heater on the CHF for saturated boiling and cited a correlation (Sadasivan and Lienhard, 1986) as given by the following equation:

$$\frac{\Phi}{\Phi_{\text{pred}}} = 1 + 0.00002\, r^{1.7}/Fr, \tag{10}$$

where

$$\Phi = \frac{\pi q_c''}{U \rho_G h_{LG}},$$

$$Fr = \frac{U}{(2Rg)^{1/2}},$$

$$\Phi_{\text{pred}} = \alpha + \left[ \frac{4\alpha^2}{We_G} \left( 1 - \sqrt{\Phi_{\text{pred}}(\Phi_{\text{pred}} - \alpha)} \left( \frac{We_G}{6\alpha^3} \right)^{1/4} \right) \right]^{1/3},$$

$$We_G = \frac{(2R)\rho_G U^2}{\sigma},$$

$$\alpha = 0.077\, r^{0.314}\, We_G^{-0.12},$$

$$r = \frac{\rho_L}{\rho_G}.$$

In the above, $R$ and $U$ are the radius of the cylinder and the flow bulk velocity, respectively. This correlation worked well for many published experimental results. In order to compare the data in our study to Eq. (10), the present experimental subcooled boiling CHF value for each flow rate was converted to the value at saturated boiling by using Eq. (2). Fig. 3 shows the correlation curve, the present experimental results, and the data obtained by other researchers. Based on Fig. 3, we believe that our experimental system was performing correctly.

Boiling curves at flow rates of 0, 7.8, 14, 22 and 30 cm/s have been obtained from our experiment. These curves were plotted together in a single figure, shown in Fig. 4. It is seen that the forced convection would shift the boiling curves upward generally even though this effect is not significant in the single-phase region and nucleate boiling region. The CHF value is affected by the flow rate significantly, which implies that the introduction of a higher flow rate would increase heat transfer near the CHF effectively. The presence of forced convection also effectively improve the transition and film boiling heat transfer.

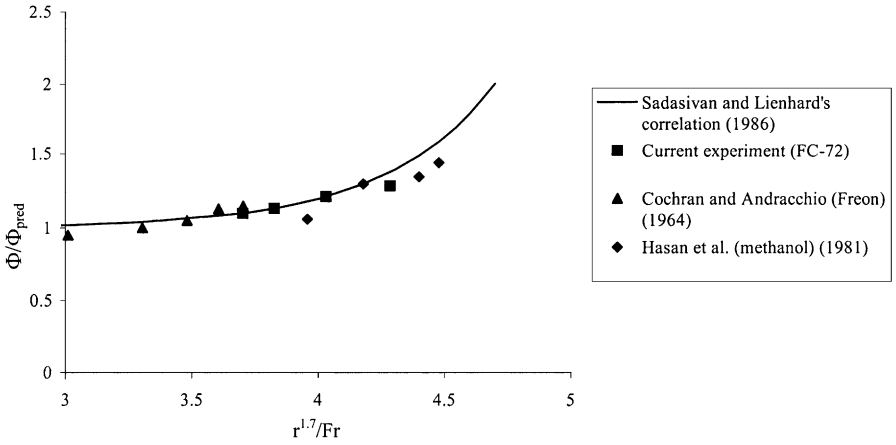


Fig. 3. Comparison of CHF in forced-convection boiling with correlation and data.

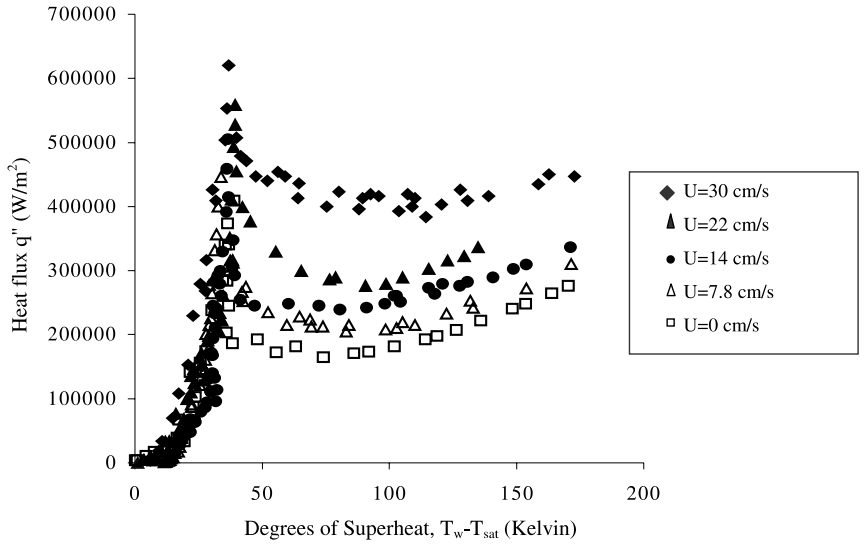


Fig. 4. The effect of forced convection on boiling curve in terrestrial gravity.

### *4.3. Forced-convection microgravity boiling*

In this study, the temperature of the heater was controlled to stay at a constant value. As a result, the heat flux from the heater surface would vary with the conditions in the fluid phase. The time-dependent variations of heat fluxes in normal gravity and microgravity for various flow rates were investigated. Fig. 5 shows a typical heat flux vs. time plot which was performed at the flow rate of 22 cm/s for transition boiling (supreheat = 51.3 K). The upward arrow ↑ means the beginning of microgravity condition, and the downward arrow ↓ means the end of it. The microgravity period lasted about 2.1 s. As shown in Fig. 8, we note that it only took a small fraction of a second for the heat flux to settle to a new level when the microgravity condition went into

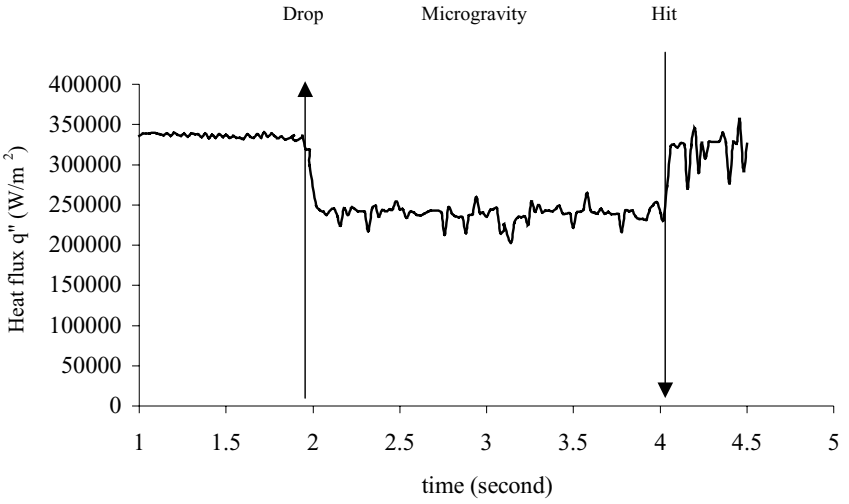


Fig. 5. Flow boiling process in WSU 2.1-s drop tower at superheat 51.3°C ($U = 22$ cm/s).

effect. This suggests that the microgravity time period for the present experiments is adequate. It is also worth noting that the heat flux level was very stable before the drop which assured that the 3-s heating period was long enough to establish a steady condition before the experiment was dropped.

Microgravity boiling experiments are difficult and very time consuming. Therefore, the terrestrial experiments became very useful in helping determine the best way to utilize microgravity experimentation time. Data were collected around the region of CHF for three different flow rates: 7.8, 22 and 30 cm/s.

Fig. 6 shows the forced-convection microgravity boiling results for the flow rate of 22 cm/s, which is plotted together with the forced-convection terrestrial gravity results in a standard boiling curve format. It was found that the boiling curve for microgravity was downward shifted as compared with that for the terrestrial gravity. For the three flow rates, we found that the difference between microgravity and terrestrial gravity is larger as the flow rate is decreased, which implies that when the flow rate is increased, the effect of microgravity is decreased. Fig. 7 contains exclusively microgravity data for all three flow rates. The curve corresponding to the highest flow rate lies above the other two. This trend is similar to that in terrestrial gravity. Fig. 8 shows the CHF comparison between terrestrial gravity and microgravity. The flow rates were non-dimensionalized by the Reynolds number which is defined as follows:

$$Re = \frac{UD}{v}. \tag{11}$$

In Fig. 8, it was found that the CHF in microgravity is lower than that in terrestrial gravity. However, when the flow rate is increased, the two lines tend to approach each other. This phenomenon suggests that the CHF values in terrestrial gravity and microgravity would be similar in magnitude if the flow rate reaches a certain value. In other words, the gravity level would be irrelevant when the forced-convection achieves dominance.

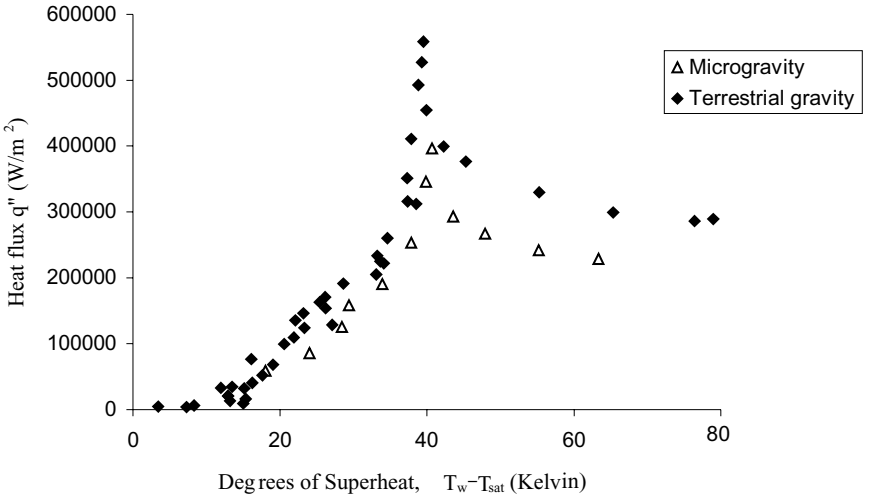


Fig. 6. Forced-convection driven terrestrial gravity and microgravity boiling curves for FC-72 at $U = 22$ cm/s.

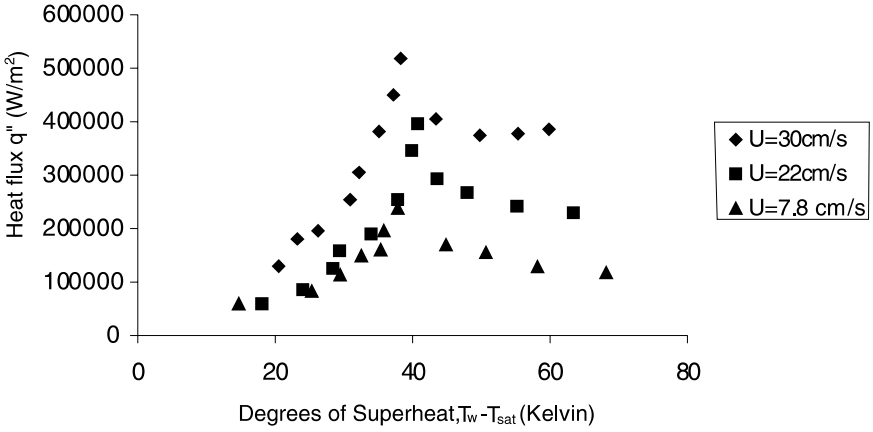


Fig. 7. Forced-convection driven boiling curves of FC-72 in microgravity at various flow rates.

It is interesting to note that for pure pool boiling the heat transfer was found to be higher in microgravity than that on earth (Weinzierl and Straub, 1982). We suggest that it is possibly due to the transient effects and g-jitters. Pool boiling in microgravity is intrinsically an unsteady process because the bubbles generated are not removed. In the experiment of Weinzierl and Straub (1982), a lot of random motion for the bubbles due to disturbances or g-jitters was seen which enhances the heat transfer. In a recent paper, Lee et al. (1997) reported results from a microgravity pool boiling experiment on a Space Shuttle. They presented a boiling curve which shows that in microgravity, the heat transfer is higher than terrestrial value for low heat flux nucleate boiling while the terrestrial heat transfer is much higher for high heat flux nucleate boiling. In general, their heat transfer data for microgravity are relatively on the same order of magnitude irrelevant of heater surface temperature which indicates that the dominant resistance is in the fluid phase due to the

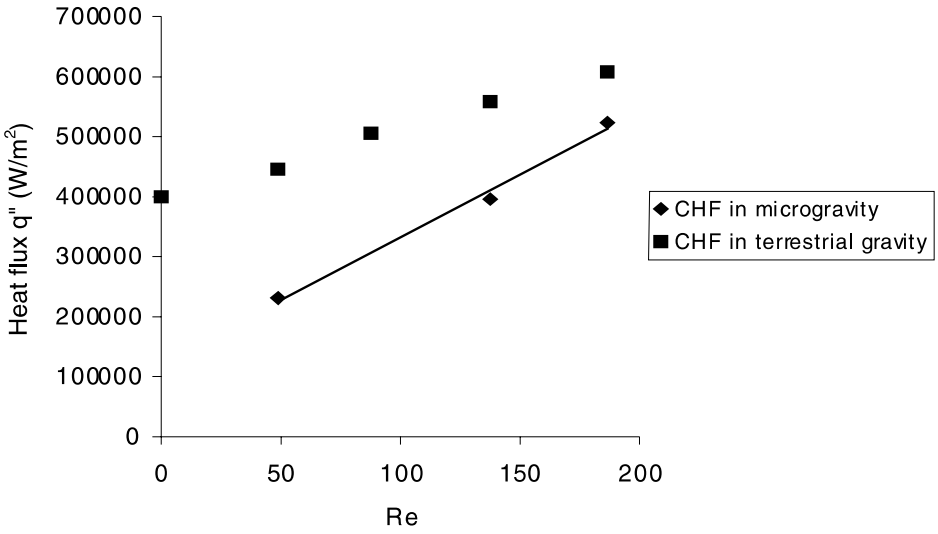


Fig. 8. Comparison of CHF data for forced-convection driven terrestrial gravity and microgravity boiling.

accumulation of bubbles. We believe that it is also the transient effects that resulted in higher microgravity heat transfer for the low heat flux cases in the experiment of Lee et al. (1997). For the forced-convection boiling in the present paper, the flow provides the mechanism for bubble removal and maintaining the steady state. Fig. 8 provides the verification for the steady condition achieved in our experiment.

### 4.4. Boiling visualization

To obtain more information on boiling bubble dynamics, video recordings that show a top view of the heater were conducted. Figs. 9 and 10 provide typical terrestrial boiling bubble images on the heater at different flow rates ranging from 7.8 ($Re = 48.8$) to 22 ($Re = 137.6$) cm/s. In these figures, the flow direction is from right to left.

In terrestrial gravity, when the flow rate was relatively low ($Re = 48.8$ and 87.6), small bubbles did not coalesce and kept the spherical shape when heater surface temperature was low. In Fig. 9(a), it is shown that all the bubbles were generated at the downstream side of heater because the temperature there is higher than that at the upstream side due to the flow effect. When the heater temperature was increased, the bubbles' sizes increase significantly and part of them would coalesce, as shown in Fig. 9(b). At the upstream side of heater surface, some small bubbles would form. As the heater temperature was increased further more, film boiling took place. The bubbles' shapes are no longer spherical but tending to become oblate and the base portion of each bubble is attached to a thin vapor layer that covers the heater surface, as shown in Fig. 9(c). However, the vapor layer thickness is not uniform along the heater surface due to instability. It was found that the vapor layer on the downstream side of heater was thicker. For higher flow rate cases ($Re = 137.6$ and 186.7), the bubbles were smaller for nucleate boiling as shown in Fig. 10(a). The reason lies in the fact that the high flow rate convects more heat away from the surroundings of bubbles so that bubble growth was suppressed. When the heater temperature increased further, it

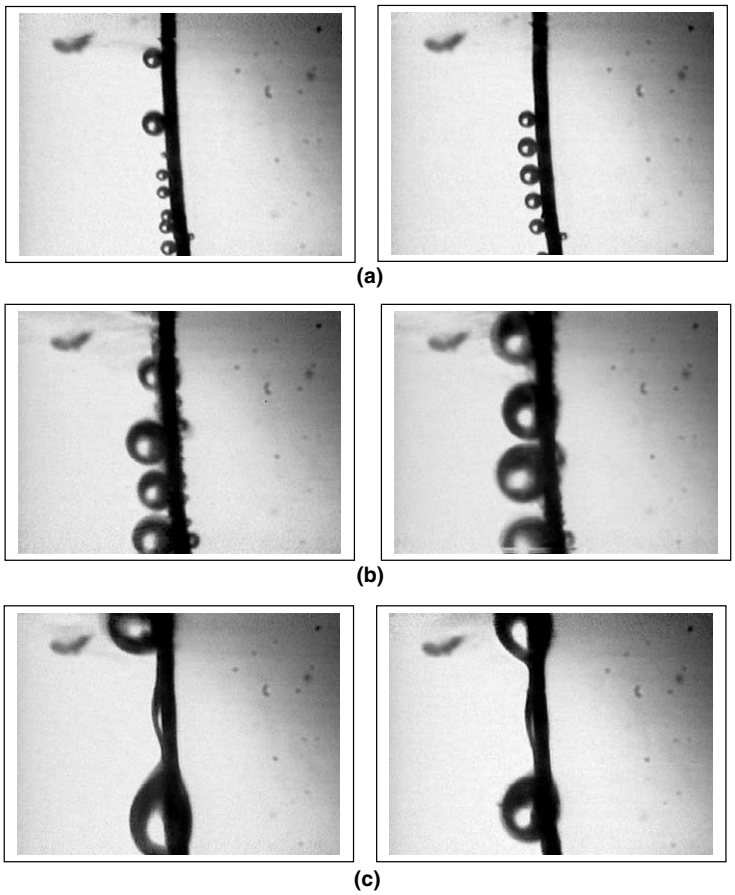


Fig. 9. Forced-convection driven boiling in terrestrial gravity ($U = 7.8$ cm/s, $Re = 48.8$): (a) $\Delta T = 13°C$, $q'' = 30{,}000$ W/m$^2$; (b) $\Delta T = 107°C$, $q'' = 22{,}000$ W/m$^2$; (c) $\Delta T = 227°C$, $q'' = 370{,}000$ W/m$^2$.

was observed that part of the heater was occupied by a vapor layer which feeds to a long tail toward the downstream side of flow, as shown in Fig. 10(b). From the experimental data, we found that the boiling is in the transition boiling regime when the tails start to present. It is interesting to note that the boiling pattern is different from those for the low flow rates. If the heater temperature continues to increase, the entire heater surface was covered by a vapor layer and no bubbles could be seen. The vapor layer tail seems not stable, but generally the tail length is longer for higher heater temperature. These phenomena of film boiling are shown in Fig. 10(c).

Figs. 11 and 12 show the microgravity boiling on the wire heater at flow rates of 7.8 and 22 cm/s. In these figures, the flow direction is from right to left.

For the lower flow rate ($Re = 48.8$) case, the bubbles on the heater surface for relatively low heater temperature is similar to the case in terrestrial gravity. The expected bubble coalescence and vapor layer formation was not observed. This implies that the flow effect is strong enough to overcome the microgravity effect for the low heater temperature case. When the heater surface temperature increases, the bubbles in microgravity would coalesce and form a bigger bubble as

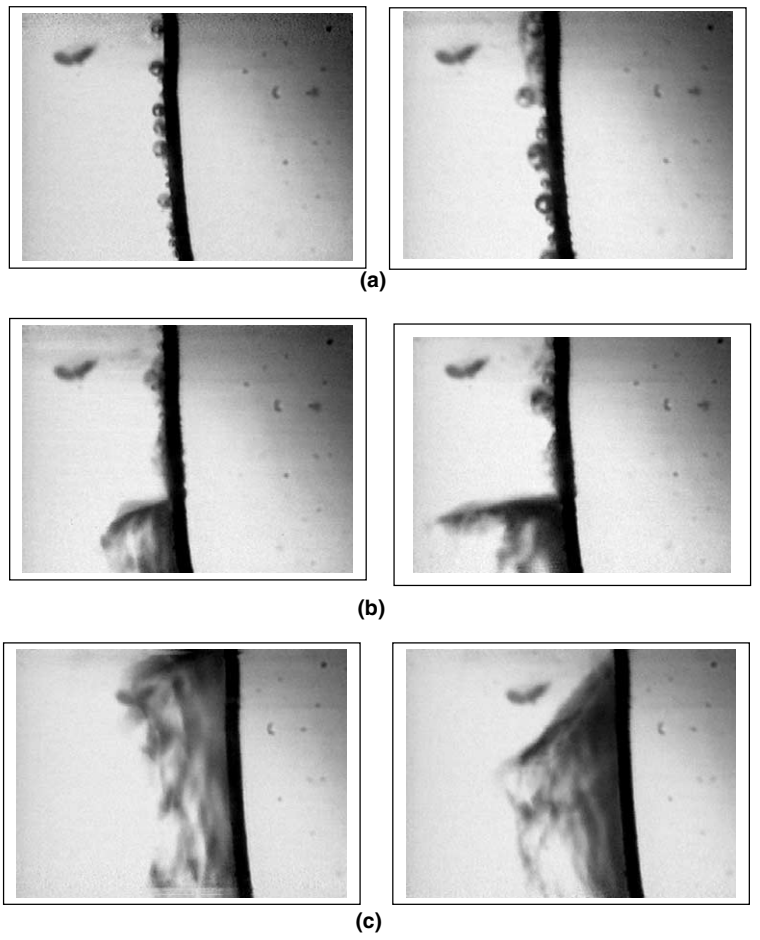


Fig. 10. Forced-convection driven boiling in terrestrial gravity ($U = 22$ cm/s, $Re = 137.6$): (a) $\Delta T = 23°C$, $q'' = 125{,}000$ W/m$^2$; (b) $\Delta T = 78.6°C$, $q'' = 280{,}000$ W/m$^2$; (c) $\Delta T = 82.7°C$, $q'' = 275{,}000$ W/m$^2$.

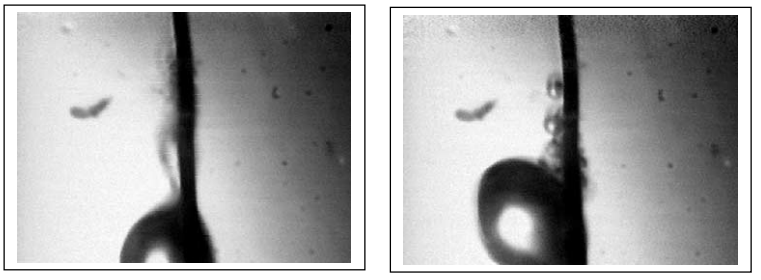

Fig. 11. Forced-convection driven boiling in microgravity ($\Delta T = 26°C$, $q'' = 95{,}000$ W/m$^2$, $U = 7.8$ cm/s, $Re = 48.8$).

shown in Fig. 11. This phenomenon was not observed in terrestrial gravity. This might be caused by the increased heater temperature which provides more heat to facilitate the formation of large bubbles before their departure. If the heater temperature keeps increasing to the film boiling

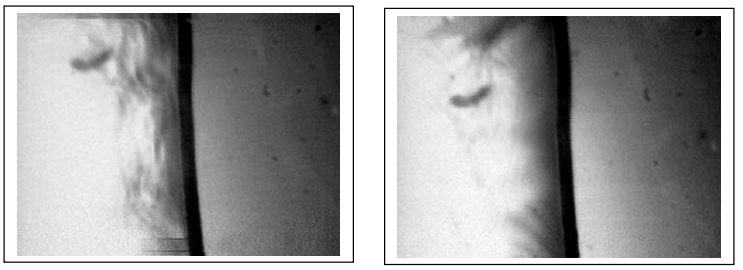

Fig. 12. Forced-convection driven boiling in microgravity ($\Delta T = 55°C$, $q'' = 230{,}000\ W/m^2$, $U = 22$ cm/s, $Re = 137.6$).

regime, it was found that the vapor layer with a long tail was formed and the tail length is similar to that in terrestrial gravity, as shown in Fig. 12. This again confirms that at high flow rates the difference between terrestrial gravity and microgravity would diminish.

## 5. Conclusion

1. The CHF in flow boiling increases with increasing flow rates in terrestrial gravity and boiling curves shifts upward when the flow rate is increased. The results agree well with the correlation given in Sadasivan and Lienhard (1986). The flow effectively improves the transition and film boiling heat transfer.
2. In microgravity flow boiling, the CHF phenomenon was also investigated. In general, the heat transfer was lowered in microgravity especially at the CHF and during transition boiling. As expected, the difference between microgravity CHF and terrestrial gravity CHF decreased as the flow rate was increased.
3. The forced convection enhances heat transfer in microgravity. In the nucleate boiling regime, higher flow rate increases the heat transfer significantly. In the transition boiling regime, even the medium level forced convection causes a significant increase in heat transfer.
4. From visualization results, it was found that the bubbles stay isolated from one another for lower heater temperature in both terrestrial gravity and microgravity. When the heater temperature was increased, the bubble shape changes from spherical to oblate and bubbles tend to coalesce.
5. In the film boiling region, a vapor layer covered the entire heater surface. However, the pattern of this vapor layer is not the same between lower flow rate and higher flow rate. In the lower flow rate field, the vapor layer is thin and distinguishable. Bubbles could be seen as part of the vapor layer. In the higher flow rate field, there are no apparent bubbles and a thick vapor zone with a long tail was observed.

## Acknowledgements

This material is based on work supported by NASA under Grant No. NAG3-1387 and Dr. Fran Chiaramonte was the grant monitor, who provided constant support to our project.

Financial support from the Andrew H. Hines, Jr./Florida Progress Corporation Endowment fund is appreciated.

## References

Churchill, S.W., Chu, H.S., 1975. Correlating equations for laminar and turbulent free convection from a horizontal cylinder. Int. J. Heat Mass Transfer 18, 1049–1053.

Haramura, Y., Katto, Y., 1983. A new hydrodynamic model of the critical heat flux, applicable widely to both pool and forced convective boiling on submerged bodies in saturated liquids. Int. J. Heat Mass Transfer 26, 389–399.

Ivey, H.J., Morris, D.J., 1966. Critical heat flux of saturation and subcooled pool boiling in water at atmospheric pressure. In: Proc. 3rd Int. Heat Trans. Conf. vol. 3, pp. 129–142.

Keshock, E.G., Siegel, R., 1964. Forces acting on bubbles in nucleate boiling under normal and reduced gravity conditions. NASA TN D-2299.

Kutateladze, S.S., 1948. On the transition to film boiling under natural convection. Kotloturbostroenie 3, 10–18.

Lee, H.S., Merte, H., Chiaramonte, F., 1997. The pool boiling curve in microgravity. J. Thermophys. Heat Transfer 11, 273–283.

Lienhard, J.H., 1988. Burnout on cylinders. J. Heat Transfer 110, 1271–1286.

Ma, Y., 1998. Forced convection boiling heat transfer in terrestrial and microgravity environments. Ph.D. Dissertation, School of Mechanical and Materials Engineering, Washington State University.

Ma, Y., Chung, J.N., 1998. An experimental study of forced convection boiling in microgravity. Int. J. Heat Mass Transfer 41, 2371–2382.

Merte, H., Lee, H.S., Ervin, J.S., 1993. Transient nucleate pool boiling in microgravity – some initial results. In: Int. Symp. on Microgravity Science and Applications, paper J-5.

Moehrle, M., 1977. Terrestrial and microgravity pool boiling heat transfer and critical heat flux phenomenon in an acoustic standing wave. M.S. Thesis, School of Mechanical and Materials Engineering, Washington State University.

Rule, T.D., 1997. Design, construction, and qualification of a microscale heater array for use in boiling heat transfer. M.S. Thesis, School of Mechanical and Materials Engineering, Washington State University.

Sadasivan, P., Lienhard, J.H., 1986. Burnout of cylinders in flow boiling: the role of gravity influences on the vapor plume. In: ASME/AIChE Heat Transfer Conf., Pittsburgh, PA.

Stephan, K., Abdelsalam, M., 1980. Heat-transfer correlations for natural convection boiling. Int. J. Heat Mass Transfer 23, 73–87.

Usiskin, C., Siegel, R., 1961. An experimental study of boiling in reduced and zero gravity fields. J. Heat Transfer 83, 243–253.

Weinzierl, A., Straub, J., 1982. Nucleate pool boiling in microgravity environment. In: Proc. 7th Int. Heat Transfer Conf.

You, S.M., Simon, T.W., Bar-Cohen, A., 1990. Experiments on nucleate boiling heat transfer with a highly wetting dielectric fluid: effects of pressure, subcooling and dissolved gas content. In: ASME Cryo. & Immersion Cooling of Optics and Elect. Equip. Conf., HTD-131, pp. 45–52.

You, S.M., Simon, T.W., Bar-Cohen, A., Hong, Y.S., 1995. Effects of dissolved gas content on pool boiling of a highly wetting fluid. J. Heat Transfer 117, 687–692.

Zuber, N., 1958. On the stability of boiling heat transfer. J. Heat Transfer 80, 711–723.